EARTH SCIENCES
RESEARCH JOURNAL

Earth Sci. Res. J. Vol. 11, No. 2 (December 2007): 117-130

GEOMETRIC MODEL OF THE NAZCA PLATE SUBDUCTION IN SOUTHWEST COLOMBIA

Patricia Pedraza Garcia[1], Carlos Alberto Vargas[1] and Hugo Monsalve J.[2]

[1] M.Sc in Geophysics, Universidad Nacional de Colombia – Bogotá, Colombia
e-mail: patriciapedrazag@gmail.com; e-mail: cavargasj@unal.edu.co

[2] CEIFI, Quimbaya Group – Universidad del Quindio, e-mail: hugom@uniquindio.edu.co

ABSTRACT

A geometric model for the subduction of the Nazca plate beneath the South American plate in southwestern of Colombia is proposed based on the relocation of hypocenters of local and distant earthquakes. By means of the simultaneous inversion of teleseismic P and SH body waves, the depths of the 15 events with Mw ≥ 5.8 were constrained, and the hypocenters of the 250 earthquakes recorded between 1990 and 2005 by the International Seismological Centre (ISC) and U.S. Geological Survey, National Earthquake Information Center (NEIC) were constrained and relocated. A model is proposed for the hypocentral sections taking into account the trench along of the Earth and Colombia-Ecuador. Three different possible shapes of subduction of the Nazca plate in the Colombia-Ecuador trench were obtained: The first configuration, in the Cali A segment, the dip angle changes from17º to 45º down to a maximum depth of 100km; the second configuration, in the Popayán B and Nariño C segments, the dip angle holds approximately constant at 30º down to a maximum depth of 200 km; and the third configuration, in the Quito D segment, the dip angle changes of 9º to 50º to a maximum depth 220 km. The maximum depth of seismicity along the Colombia-Ecuador trench shows two increases, the first between latitudes 4.5ºN-5ºN and the second between the latitudes 1ºS-2ºS, which suggest that the presence of the Malpelo and Carnegie Ridges may generate a differential blockage at the Pacific Colombia-Ecuador basin.

Key words: Seismotectonic, Nazca plate, subduction, Colombia.

RESUMEN

Se propone un modelo geométrico de la subducción de la placa Nazca bajo la placa suramericana en el suroeste de Colombia, basado en la relocalización de hipocentros de sismos locales y telesismos. Mediante la inversión simultánea de formas de ondas internas P y SH telesísmicas se ajustan las profundidades de 15 eventos con Mw ≥ 5.8 y se relocalizan los hipocentros de 250 eventos con lecturas de fases registradas desde 1990 hasta 2005 por las agencias International Seismological Centre (ISC), y U.S. Geological Survey, National Earthquake Information Center (NEIC). Se propone

Manuscript received March 13 2007.
Accepted for publication November 20 2007.

un modelo de secciones hipocentrales teniendo en cuenta la curvatura de la Tierra y la curvatura de la fosa Colombia-Ecuador. Se obtienen tres formas distintas de subducción para la placa Nazca en la fosa Colombia-Ecuador: La primera en el segmento Cali A, donde él ángulo de buzamiento cambia de 17º a 45º, a una profundidad máxima de 100km, la segunda en los segmentos Popayán B y Nariño C donde el ángulo de buzamiento es aproximadamente constante de 30º a una profundidad máxima de 200km y la tercera en el segmento Quito D donde el ángulo de buzamiento cambia de 9º a 50º a una profundidad máxima de 220km. La profundidad máxima de sismicidad a lo largo de la fosa Colombia-Ecuador presenta dos aumentos, el primero entre las latitudes 4.5ºN-5ºN y el segundo entre las latitudes 1ºS-2ºS, sugiriendo la presencia de las dorsales de Malpelo y Carnegie que generan un bloqueo diferencial respecto a la cuenca del Pacífico Colombo-Ecuatoriano.

Palabras claves: Sismotectónica, placa Nazca, subducción, Colombia.

INTRODUCTION

Southwestern Colombia is a region of enhanced tectonic activity resulting from the subduction of the Nazca Plate (NP) beneath the South American plate (SA) along the Colombia-Ecuador Trench (CET). Several studies have shown that this subduction zone may exhibit lateral variations in the dip angle of the subducted oceanic lithospere as well as changes in the distribution of seismicity along and down dip the trench, specially at intermediate depths (between the latitudes 3ºN-4ºN), where a seismic gap is apparent (Pennington, 1981; Taboada *et al*., 1998; Monsalve, 1998; Gutscher *et al*., 1999, Vargas *et al*., 2003, Mejía and Meyer, 2004, Chicangana and Vargas, 2004).

Pennington (1981) obtained contours for the Wadati-Benioff Zone (WBZ) beneath northwestern South America and determined three segments with different directions and dip angles: the Bucaramanga segment from 5.2ºN to 11ºN, which is subducting in direction N109ºE and with dip of 20º-25º; the Cauca segment in the Colombia-Panama trench from 7ºN to 1.5ºN, which is subducting in direction N120ºE and dipping approximately 35º; and the Ecuador segment in the CET from 1.5ºN to 2ºS, which is subducting in direction N35ºE and a dipping approximatly 35º.

The direction of the Ecuador segment can be explained by a speculative model related with the activity of the Galápagos hot spot. This hot spot is located some 100 km to the south of the presently active Cocos-Nazca plate spreading center and could be subducting beneath the south of Ecuador near 1ºS-2ºS. This bathimetric feature could be the cause of the low subduction angle at the Peru-Ecuador border (Barazangi and Isacks, 1976). A more recent study made by Gutscher *et al*. (1999) shows a more complex behavior of the plate with the conclusion that the Ecuadorian system of subduction seems highly controlled by the subduction of the Carnige Ridge and by the rupture of the lithospere within the NP.

Mejía and Meyer (2004) based on the seismological information compiled by the Observatorio Sismológico del Suroccidente-OSSO propose a transition zone between active subduction and a possible blocked subduction by the addition of the Choco Block to the western coast of Colombia. Recent GPS measurements from the CASA project (Central and South America), reveal a wide plate boundary deformation with escape tectonics occurring along an approximate length of 1400 km of the North Andes, locking of the subducting NP and strain accumulation in the Ecuador-Colombia forearc (Trenkamp *et al*., 2004)

.

Associated with the process of subduction of the NP there is a volcanic arc, that extends

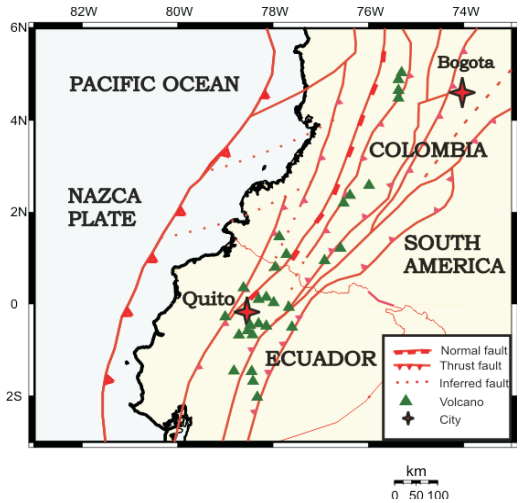

Figure 1. General tectonic setting of the study area.

from 5ºN (Cerro Bravo Volcano, Colombia) to 2ºS (Sangay Volcano, Ecuador). The SE active volcanism only reappears in Perú. The subducted oceanic crust, with ages between 12 and 20 Ma, is carrying the Carnegie Ridge, which is composed of volcanic products from the activity of the Galápagos hot spot on the NP and that has been subducting for at least 6 Ma. (Hey, 1977).

DATA AND METHODOLOGY

The purpose of this study is to determine the geometry of subducted NP based on all the available and reliable locations of earthquakes recorded with local and teleseismic networks, and to explain the decrease in the intermediate-depth seismicity in southwestern Colombia. Initially, some teleseismic events are constrained from the inversion of long-period body waves (Nabelek, 1984). These earthquakes are used as calibration events to relocate local events by means of the Joint Hypocenter Determination-JHD method (Dewey, 1971). Hypocentral cross-sections are tipically presented as straight cross-sections in different studies at the Middle and South American Trenches (Isacks *et al*., 1968; Isacks and Barazangi, 1977; Pennington, 1981 Burbach *et al*., 1984, Vargas *et al*., 2003) but more recent works such as those by Kawatsu (1986), Ekstrom and Engdhal (1989), Guzmán (1995), and Monsalve (1998), consider the arc-trench and Earth curvatures, demonstrating a better definition of the WBZ.

Data used in the inversion of body wave

Earthquakes of events with Mw ≥ 5.8 reported by NEIC-USGS (National Earthquake Information Center) for the 1990-2005 period were selected. The Digital registries of the teleseismic P and SH body waves were provided by IRIS-DMC (Incorporated Research Institutions for Seismology) agency.

Digital records of P and SH waveforms with periods between 1s and 100s were analyzed. The data used corresponded to waveforms recorded by broadband stations with a good azimuthal coverage located at distances from 30º to 90º to avoid the effects of the Earth's core and upper mantle discontinuities on the waveforms. Figure 2 shows the location of the stations used in this study. The instrument response was de-convolved from the traces and the waveforms integrated to obtain

displacement amplitudes.

The amplitudes were normalized for a magnification of the instrument equal to one and an epicentral distance of 40 degrees in order to unify the data. The waveforms are band-pass filtered with a three pole Butterworth filter with cutoffs at 0.01Hz and 1Hz to eliminate long and short period noises respectively.

Synthetic seismograms were generated by a combination of the direct (P or S) and reflected (pP and sP, or sS) phases radiated from a linear source (Bouchon, 1976) using the BWIDC computer program developed by Nabelek (1984). This program is based on the minimization, in the least square sense, of the misfit between observed and synthetic seismograms. The synthetic seismogram at each station is obtained by the convolution of Green's function with the instrumental response and the source time functions. The source time function is parameterized as a single point source or as an event composed of several point sources separated in time and space depending on the complexity of the event. Weights were assigned to the stations according to azimuthal density of the data.

$\frac{1}{\sqrt{N}}$ for P waves and $\frac{1}{\sqrt{2N}}$ for SH waves were used, where N is the number of stations to avoid the uprising situations from a poor azimuthal cover.

Table 1a Velocity model near the sources (INGEOMINAS, 1993)

Thickness (km)	α (km/s)	β (km/s)	ρ (gr/cm^3)
2.0	4.0	2.3	2.57
3.0	5.5	3.18	2.84
20.0	6.4	3.70	2.95
10.0	7.1	4.10	3.04
∞	8.1	4.68	3.30

Note: α= P- wave velocities; β= S-wave velocities; ρ=densities

Table 1b. Velocity model for the crust in the receiver region

Thickness (km)	α (km/s)	β (km/s)	ρ (gr/cm^3)
60.0	6.0	3.46	2.57
∞	6.0	3.46	2.57

Note: α= P- wave velocities; β= S-wave velocities; ρ=densities

Table 1a and 1b show the model of velocity structure for the crust near the source proposed by INGEOMINAS (1993) and assumed in this paper. The anelastic attenuation along the propagation path was parameterized using an attenuation value of t* =1s for P waves and a t* =4s for SH waves.

Data used in the relocated earthquakes

Earthquakes with magnitude $m_b \geq 3.5$ in southwestern of Colombia were relocated using the JHD method (Dewey, 1971) and the phases readings reported by ISC and NEIC between 1990 and 2004 used. This was done as an effort to reduce the errors in the hypocentral locations determined by ISC and NEIC, since this method permits a better constrained estimate of the focal depth when a considerable number of pP phases are included. The JHD method determines the location of a set of earthquakes, applying time adjustments with a least squares estimation for the P, pP, and S phase readings, using the time interval between pairs of phases. The 2004 Pizarro-Colombia earthquake (Mw=7.2) was used to calibrate the event, along with 14 earthquakes with fixed depths by means of a teleseismic body waveform inversion.

RESULTS AND DISCUSSION

Body waveform inversion

In this study, 15 events with a reported Mw≥ 5.8 magnitude between 1990 and 2005 were modeled. These earthquakes are the most representative of the seismicity in the Colombia-Ecuador zone and cover, in a relatively homogenous way, the Colombia-Ecuador subduction zone. Ten of the selected earthquakes have shallow hypocentral depths

(h≤70km), one earthquake has an intermediate hypocentral depth (70km≤h≤140km), and four earthquakes have deep hypocentral depth (h>140km). The results of the inversion of body waves of this events are summarized in the table 2, and an example of the focal mechanisms, waveform, and source time functions modeled are shown in Figure 3 along with a comparison between the observed records (solid lines) and synthetic seismograms (dashed lines). The focal mechanism and the relative location of the teleseismic stations are shown on the lower focal hemisphere.

Table 2. Earthquake Hypocentral and Fault Plane Solution Data obtained in this study. All events were relocated using JHD method (Dewey, 1971).

Hypocentral sections

The Colombia-Ecuador Trench (CET) may be divided into segments of constant curvature, which represent arcs or small circles on a sphere. By means visual inspection, two arcs along the CET were identified (Figure 1). For each arc, a center of curvature most closely fitting was obtained by using the GMT mapping programs (Wessel and Smith, 1991). An arc is concave towards the ocean and it extends approximately from 78ºW to 79ºW in a NW-SE direction. In front of the Colombia-Ecuador boundary, the curvature center is roughly located at 6.387ºN, 82.781ºW, and at a distance of approximately 504km, and other arc is concave towards the continent with the same general NW-SE direction, and goes from 79ºW to 81,6ºW to the southeastern end of the study zone, the center of curvature is located at 4.016ºS, 69.984ºW at a distance of approximately of 723km.

These segments were divided into two parts each one, according to the distribution of the seismicity (Figure 4). Perpendicular hypocentral projections and along the arc were done following the propose methodology by Guzman, S (1995). In this methodology, for the sections perpendicular to the arc, the hypocenter are project as a function of their latitude with respect to the pole and or depth, holding constant their longitude with respect to the pole and for projection along the arc, the hypocenter are projected onto the arc as a function of their longitude an depth with respect to the pole, that is, through great circles from the pole to the arc then this surface is projecting onto a plane (Figure 5). The position of the trench in cross-section view is always located in the upper-left corner of the section.

Focal mechanims

In this study, 15 focal mechanisms are modeled by means of inversion of P and SH body waveform and 14 mechanisms are CMT solutions reported by the Harvard University. All events were relocated with the JHD method (Figure 7a). These focal mechanisms are also shown on lateral projections on the cross sections (Figure 5). In Figure 7b, the focal mechanisms reported by Harvard University (but not relocated) are shown.

In a analogous manner to the seismicity, the stress pattern observed along the subduction zone may be divided in three zones: two zones where the mechanisms correspond to a compressional regime (thrust faulting), the first one from 5ºN to 4ºN, and the second one from 1.5ºN to 2ºS, and a third zone from 4ºN to 1.5ºN where a variety of mechanisms are observed: Normal, thrust, and strike-slip, which is something unexpected for shadows subduction. A possible explanation to this behavior is a folding of the subducted plate due to a blockage possibly caused by the subducted Malpelo and Carnegie Ridges within the Cali A and Quito D segments respectively.

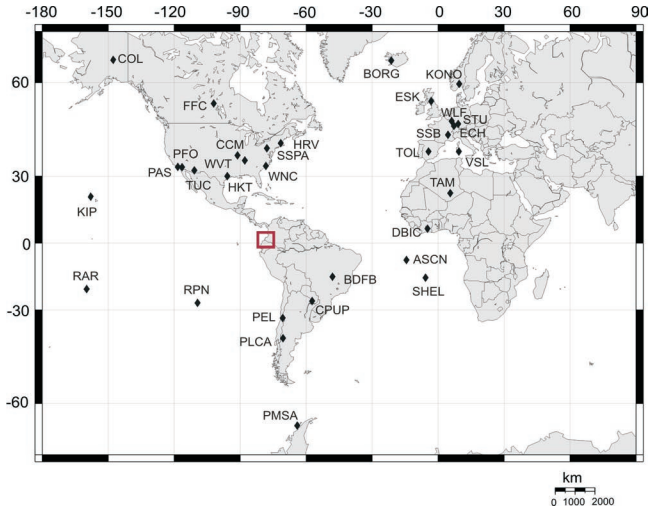

Figure 2. Location of seismograph stations used in this study.

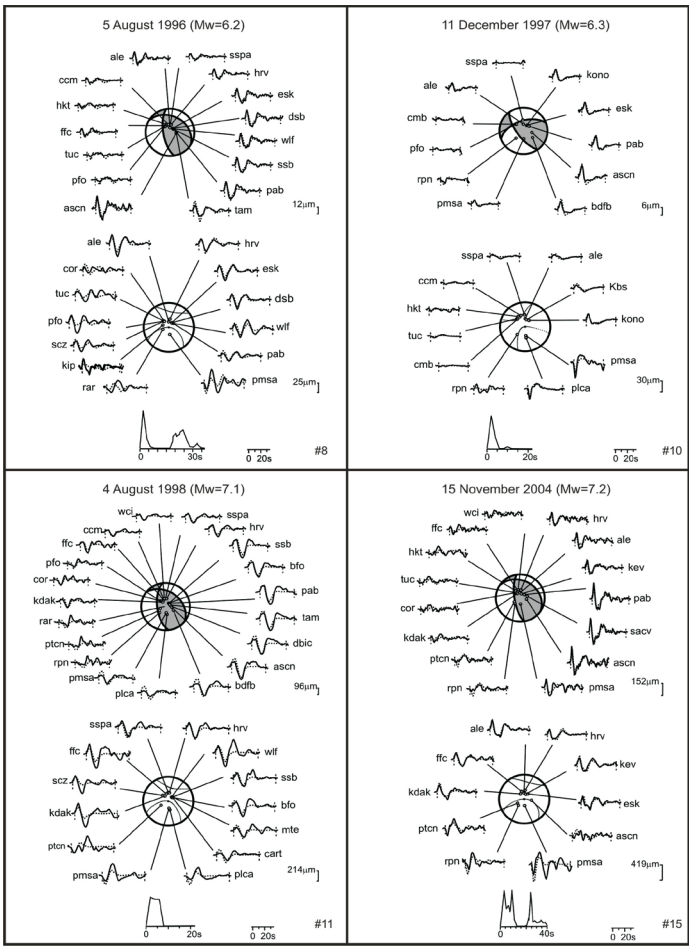

Figure 3. Plot of P (top) and SH (bottom) waveforms for 4 selected earthquakes representative of the data and their inferred focal parameters. Solid lines are observed records and dashed lines are the synthetics records. Also shown are their corresponding source time functions. Time and amplitude scales for both the P an SH waves are shown in the low part of each figure.

The intermediate seismicity is scarce and only two focal mechanisms are obtained (numbered 23 and 24). The first one corresponds to normal faulting and located at 4ºN in front of Buenaventura, Colombia, and the second one corresponds to inverse faulting and is located at 0.5ºS in front of Manta, Ecuador. The deep earthquakes are concentrated in two regions, some in the north zone between 4ºN and 5ºN and others located between 1ºS and 2ºS. For the first cluster, the focal mechanisms of two events (numbered 26 and 28) were obtained. Both mechanisms correspond to thrust faulting, with some strike-slip component, with depths ranging from 180km to 230km. In this region, tensional movements would be expected; therefore, this rupture patterns could be due to the presence of "asperities" that generate traction on a subducted slab. In the second cluster, the focal mechanisms of two events (numbered 25 and 27) are obtained and both mechanisms correspond to normal faulting.

Geometry of the subducted plate

The WBZ shows changes in its dip and maximum depth in all four segments. For the Cali segment, a change in the dip angle is considered down to a depth of 100km, to a width of approximately of 180km of the trench. Beneath the continent, it increases from 17º to 45º. A maximum depth of 220km is estimated (Figure 5). In the Popayán B segment, the dip of the WBZ decreases to 30º and reaches a maximum depth of 190km. For the Nariño C segment, the dip angle is similar to that of the Popayán B segment and with a maximum depth of 115km. In the Quito D segment, the dip angle increases of 9º to 49,5º with a depth of 100 km to a width of approximately 320km of the trench beneath the continent and to maximum depth of 220 km.

A cross section parallel to the trench from (5.5ºN, 78ºW) to (2ºS, 81.6ºW) shows a rapid variations in maximum depth of the hypocenters within southwestern Colombia (Figure 6). Two maximum depth zones are observed that correspond to the Cali A and Quito D segments. The maximum focal depth is 220 km. The depth extents of various segments of the subduction zone directly correlate with the observed dip of the slab.

Two transition zones are observed which suggest a steep change in dip angle. The first zone at 4ºN is within the Cali A segment and the second zone at 2ºS is within the Quito D segment. In the central part of the CET (3,5ºN to 1ºS), a seismic gap for intermediate and deep earthquakes is observed and the dip of the subducted slab becomes shallower (Figure 8).

In the Figure 9 a perspective view of the WBZ is shown, which is intended to demonstrate the three dimensional complexity of the Nazca plate subduction in the CET. This three-dimensional surface was obtained by means of interpolation of the isodepth contours.

Several authors have suggested that the principal factors affecting the geometry of a subduction zone are the relative convergence rate, the age of the subducted slab, the absolute motion of the overriding plate, and the subduction of aseismic bathymetric features such as ridges or intraplate seamounts (e.g., Jarrard, 1986; Gorvatov and Kostoglodov, 1997).

When comparing the ages calculated using the empirical relations given by Gorbatov *et al*, (1997) with the ages reported by Atwater (1989), the age for the Popayán B (28±1 m.a). and Nariño C (17±3 m.a.) segments are within the margin of 95% of confidence of the Gorbatov relation, but the age for the Cali A (46±8 m.a.) and for the Quito D (58±7 m.a.) segments are almost twice as large. These are precisely the segments that present

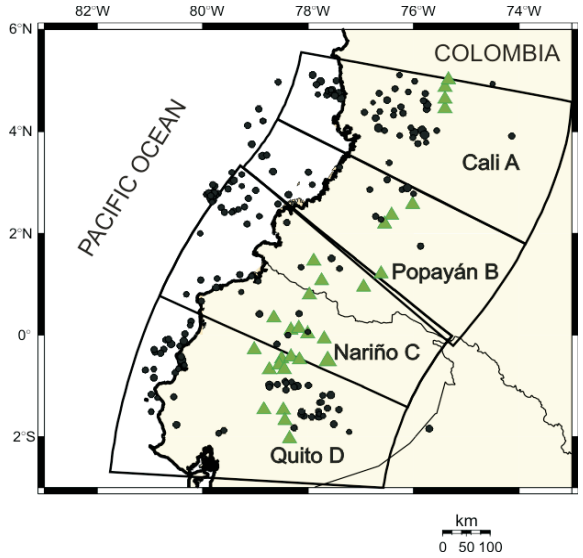

Figure 4. Hypocentral sections of the Cali, Popayan, Nariño and Quito segments. Relocated hypocenters obtained from the Joint Hypocenter Determination method (Dewey, 1971). The location of the Quaternary volcanoes (solid triangles).

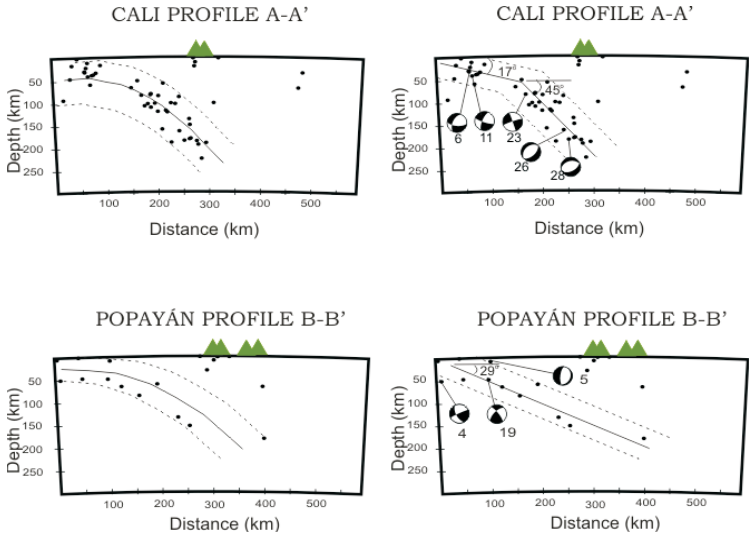

Figure 5a. Cross-sections perpendicular to the trench for the Cali A and Popayán B segments. The points mark the hypocenters relocated with JHD method, the solid line shows the tendency at depth, and the dashed line indicates the limits of the Wadati-Benioff zone.

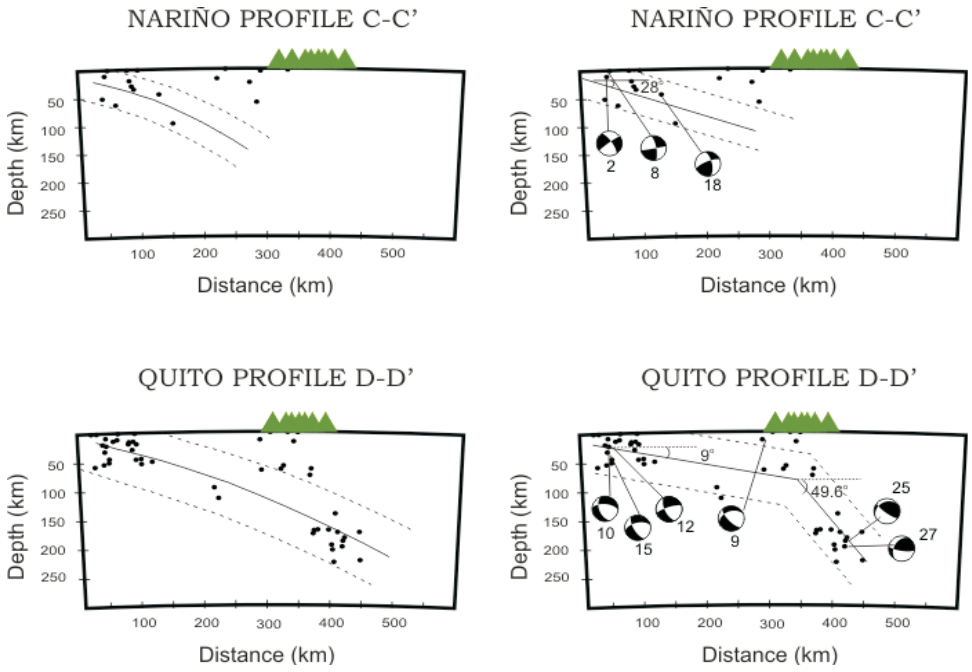

Figure 5b. Cross-sections perpendicular to the trench for the Nariño C and Quito D segments. The points mark the hypocenters relocated with JHD method, the solid line shows the tendency at depth, and the dashed line indicates the limits of the Wadati-Benioff zone.

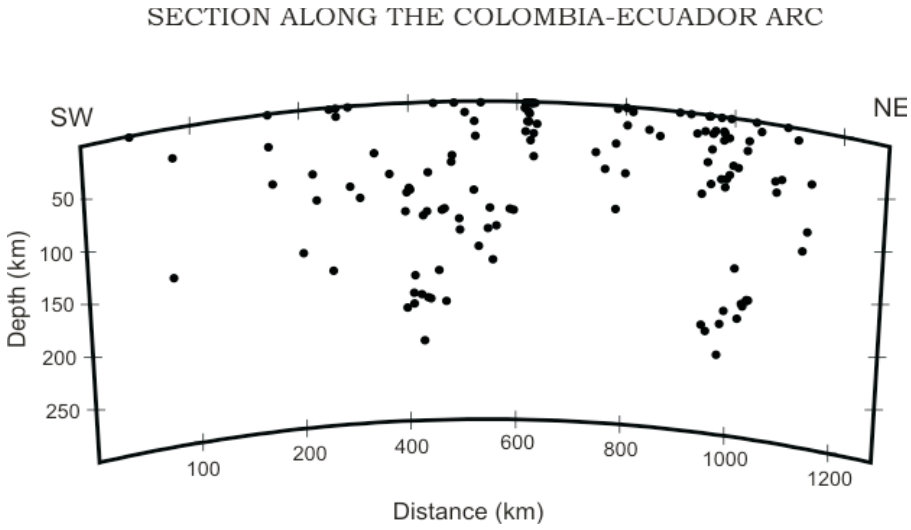

Figure 6. Cross-section along the Colombia-Ecuador arc, from (5.5N, 78W) to (2S, 81.6W). The hypocenters represented correspond to those in the catalogue of earthquakes relocated with JHD for the period 1976-2005..

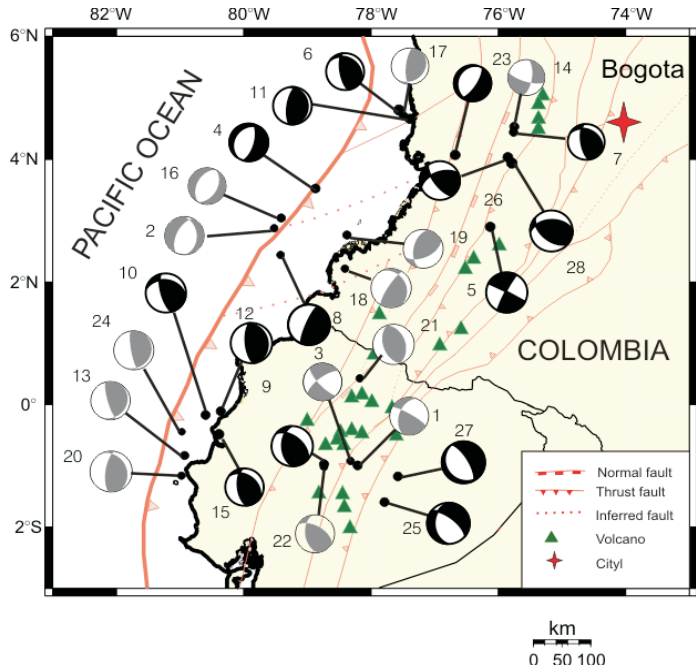

Figure 7a. Focal mechanisms of the inverted events in this study (solid) and focal mechanisms reported by the Harvard University (dashed). All events were relocated with the JHD method.

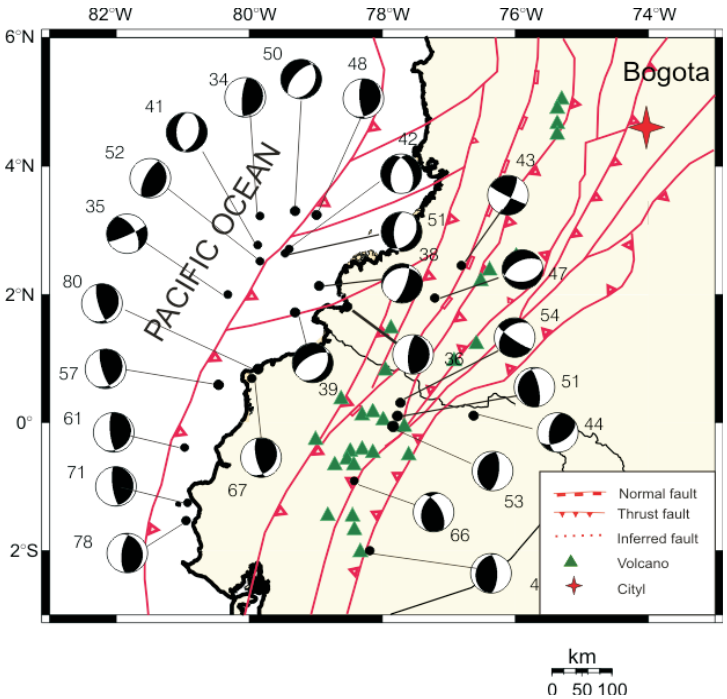

Figure 7b. Focal mechanisms reported by the Harvard University but not relocated with JHD.

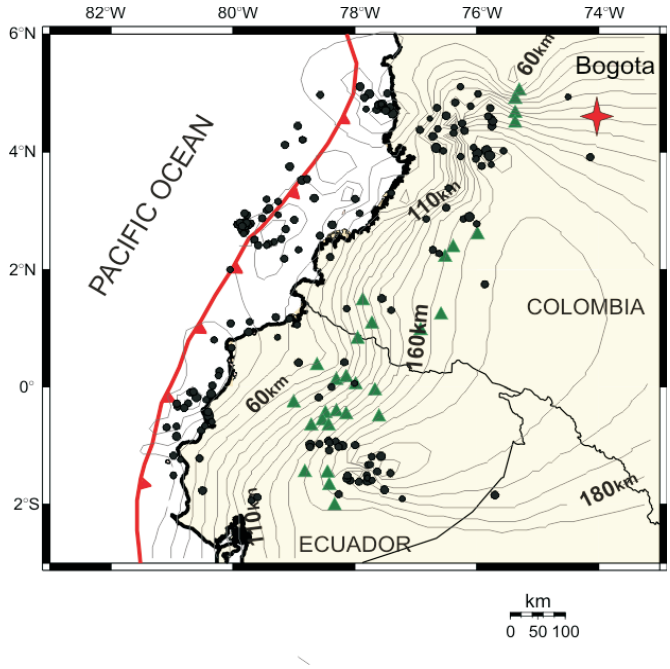

Figure 8. Isodepth contours of the subducted Nazca plate beneath the South America plate in the CET using a spline interpolation of the data relocated with the JHD method and error ellipses ≤ 20km.

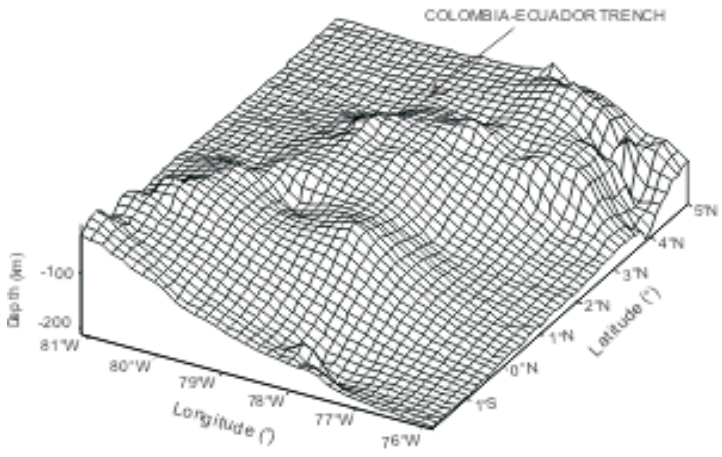

Figure 9. A three-dimensional view of the subducted Nazca plate between 5ºN and 2ºS.

changes in focal mechanisms. This situation can be explained with two hypothesis: (1) The calculated ages are the result of bias in the velocities or dip angles estimated in the present study and (2) the presence of the Malpelo and Carnegie Ridges generate differentials blockages with respect to the Colombo-Ecuatorian Pacific Basin, causing changes in the velocities of convergence in these regions.

The second hypothesis agrees with the measured vectors of convergence determined by GPS (Trenkamp *et al*., 2002) that show a change in the north component of the convergence velocities from south to north of the CET.

Other authors such as Taboada *et al*., (2000) propose an overlap zone of the Caribbean and Nazca plates located between 5,2ºN y 7ºN in Colombia. This model would explain the pronounced curve that appears in the isodepth contours in the Cali A segment between 3.5ºN-5ºN (Figure 7a). Gutscher *et al*., (1999) interpret the seismic gap at intermediate depths to the north of Ecuador between 0ºN and 1ºS to the subduction of the Carnegie Ridge and the changes in the dip angle in the Transition zones as tearing of the Nazca plate.

CONCLUSIONS

The body waveform inversion of 15 telesismic events and the relocation of 250 hypocenters detected during more than 30 years, allowed an approach to the problem or determination of the geometry of the Wadati-Benioff Zone, with a boundary in isodepth contours in the Colombia-Ecuador Trench.

The CET was constrained by means of Euler poles to two segments with different concavity: the first one is concave towards the Pacific Ocean located between 5ºN and 3.5ºN and the other one is concave towards the continent between 3.5ºN and 2ºS. Two hypocentral sections for each segment were considered.

The subduction process of the Nazca plate beneath the South America plate is constrained from the seismicity distribution within the CET. Three different subduction configurations were observed: The first in the Cali A segment, with maximum depth of 290km to 300km up to a distance of 300km from the trench and a dip angle that changes of 17º to 45º to a depth of 100 km. The second in the Popayán B and Nariño C segments with maximum depth from 130 km to 150 km up to a distance of 280km from the trench and an approximately constant dip of 30º. The third in the Quito D segment, with a maximum depth of 200km to 220km up to a distance of 430km from the trench and a dip angle that change from 9º to 50º to a depth of 80km.

The maximum depth of the seismicity of the subducted slab in the CET shows two regions of increases: the first one, from 4,5ºN to 5ºN, and the second one, from 2ºS to 1ºS. It is suggested that the presence of Malpelo and Carnegie Ridges generated a differential blockage with respect to the Colombia-Ecuatorian Pacific Basin.

REFERENCES

Atwater T. (1989). Plate tectonic History Northeast Pacific and Western North America. The Geology of North America. V. N, the Eastern Pacific Ocean an Hawaii. The Geological society of America, chapter 4.

Barazangi, M and Isacks, B.L. (1976). Spatial distribution of earthquakes and subduction of the Nazca Plate beneath South America. Geology, 4. p. 686-692.

Bouchon, M. (1976). Teleseismic body wave radiation from a seismic source in a layered medium, Geophys. J. R. Astr. Soc., 47. Pag. 515-530.

Burbach, G.V., Frohlich, C., Pennington, W.D. and Matumoto, T. (1984). Seismology and tectonics of the subducted Cocos plate. Journal Geophysical Research, 89. p. 6153-6170.

Chicangana, G. and Vargas, C. (2004). Desarrollo y Geometría actual de la Litosfera en la Esquina Noroccidental de Suramérica: First Latin -American Congress, Mem. (In CD – Room).

Dewey, J.W. (1971). Seismicity studies with the method of join hypocenter determination: Ph.D thesis, University California, Berckeley.

Ekstrom, G. and Engdahl, E. (1989). Earthquake source parameters and stress distribution in the Adak island region of central Aleutian islands, Alaska. Journal Geophysical Research, 94. Pag.15499-15519.

Futterman, W. (1962). Dispersive body waves. J. Geophysics Res., 67, 5279 -5291.

Gorbatov A and Kostoglodov, V. (1997). Maximum depth of seismicity and Thermal parameter pf the subducting slab:n general empirical relation and its application. Tectonophysics, 277. p. 165-187.

Gutscher, M.A., Malavielle, J., Lallemand, S. and Collot, J.Y. (1999). Tectonic segmentation of the North Andean margin: impact of the Carnegie Ridge collision. Earth and Planetary Science Letters, 170(1-2). Pag. 155-156.

Guzmán, S. (1995). Hypocentral cross-sections and arc-trench curvature. Geofísica International, V.34, No 1, 131-141.

Hey, R.N. (1977). Tectonic Evolution of the cocos-Nazca spresding center, Geol. Soc. Am Bull, 88, Pag. 1404-1420.

Ingeominas. (1993) Boletín trimestral Junio-Agosto.

Isacks, B., Oliver J. and Sykes L. R. (1968). Seismology and the new global tectonics. J. Geophys. Res., 73. Pag. 5855-5899.

Isacks, B.l. and M. Barazangi. (1977). Geometry of Benioff zones: Lateral segmentation and downward bending of the subducted lithosphere, In: M. Talwani and W.C. Pitman II Editors), Island arcs, deep sea trenches and back-arc basins. American Geophysical Union. Washington, 470pp.

Jarrard, R. (1986). Relations Among Subduction Parameters. Review of Geophysics. V. 24 pag. 217-284.

Kawatsu, H. (1986). Downdip tensional earthquake beneath the Tonga arc: A double seismic zone. Journal Geophysical Research, 91, 6432-6440.

Mejía, J. A. and Meyer, H. (2004). Modelo detallado preliminar de la sismicidad en el occidente de Colombia. Observatorio sismológico del Sur Occidente. OSSO. Memorias I congreso latinoamericano de Sismología. Armenia.

Monsalve, J. H. (1998). Geometría de la subducción de la Placa de Nazca en el noroeste de Colombia: Implicaciones tectónicas y sísmicas. Tesis de Maestría. Instituto de Geofísica UNAM. 107p.

Nábelek, J. L. (1984). Determination of earthquake source parameter frominversion of body waves. Thesis doctoral, Massachusets Institute of Technology.

Pennington, W.D. (1981). Subduction of the eastern Panama basin and seismotectonics of Northwestern South America. Journal Geophysical Research, V.86, 10753-10770.

Taboada, A. Dimaté, C. and Fuenzalida, A. (1998). Sismotectónica de Colombia: deformación continental activa y subducción. Física de la Tierra. Madrid, No. 10. Pag. 117-147.

Taboada, A., Rivera, L., Fuencalida, A., Cisterna, a., Philip, H., Bijwaard, H., Olaya, J. and Rivera, C. (2000). Geodynaics of the northern andes: Subductions and intracontinental deformation (Colombia). Tectonics. Vol. 19. No 5. Pag. 787-813.

Trenkamp,R., Kellogg, J., Freymuller, J. and H. Mora. (2002). Wide plate margin deformation, southern Central America and northwestern South America. CASA GPS observations. Journal of south American Earth Sciences, 15,2 p. 157-171.

Trenkamp R., Mora, H., Salcedo, E. and Kellogg, J. (2004). Possible Rapid Strain Accumulation Rates near Cali, Colombia, determined from GPS measurements (1996-2003), Earth Sci. Res. J. 8 (1), 25-33.

Vargas C.A., Pujades LL.G., Ugalde A. and Canas, J. (2003). Tomografía Sísmica Local del Territorio Colombiano. Revista Internacional de Métodos Numéricos para Cálculo y Diseño en Ingeniería. Barcelona, v.19, n.3, p.255 - 278, 2003.

Wessel, P. and Smith, H. 1998. New improved version of Generic Mapping Tools released, Trans. Am. Geophys. Union (EOS) 79, 579.